Optimal Planning of a Smart Microgrid Including Demand Response and Intermittent Renewable Energy Resources

S. M. Hakimi and S. M. Moghaddas-Tafreshi

***Abstract*—Heating/cooling systems have played an important role in building energy and comfort management. There have been intensive discussions about the integration of heating/cooling systems into the smart grid infrastructure over the past decade, yet controlling the operation of heating/cooling systems in a smart grid with high penetration of renewable resources has not been addressed clearly. This study has investigated the suitability of a novel active controller applied to heating/cooling systems in the context of smart grid with high penetration of renewable energies. The proposed controller operates by responding to a combination of internal set points and external signals (e.g. the availability of renewable energy resources and welfare of customers) from a single local controller. The heating/cooling systems management minimizes the overall cost of the simulated smart microgrid, the size of smart microgrid units, and the imported energy from the distribution grid through an optimization process. It also at the same time maximizes the reliability of the smart microgrid. Demonstrated results confirm the capability of the proposed heating/cooling system controller on the planning of a smart microgrid.**

***Index Terms*—Active controller, heating/cooling system, renewable energy, smart microgrid.**

NOMENCLATURE

$\sigma_{\text{surplus,real}}$	24–hour standard deviation of surplus power.
T_{desired}	The desired temperature set point.
T_{real}	The real temperature set point.
$T_{\min}$	Minimum acceptable temperature.
$T_{\max}$	Maximum acceptable temperature.
R_{high}	Slope between T_{desired} and $T_{\max}$.
R_{low}	Slope between T_{desired} and $T_{\min}$.
$\sigma_{\min}$	Standard deviation of surplus power corresponding to $T_{\min}$.
$\sigma_{\max}$	Standard deviation of surplus power corresponding to $T_{\max}$.
P_{surplus}	Signal representing the surplus of power.
$\text{P}_{\text{surplus,avg}}$	24 hour average of the surplus power signal.
Q_{AC}	The thermal transfer from the heating/cooling system.
Q_{loss}	The thermal loss between the indoor and outdoor environment.
m	The air mass of building area.
c_{air}	The air specific heat.
$\Delta\text{T}'_{\text{i}}$	Temperature variation at the time step i.
ρ_{air}	The air density.
V_{room}	The volume of the domestic space.
Q_{Latent}	Latent load.
ΔW	The air specific humidity.
$\text{Q}_{\text{Conduction}}$	The conduction heating load.
U	The heat transmission coefficient.
A	The Construction layer area.
CMH	The air flow infiltration rate.
R	The thermal resistance of structure layers.
X	The layer thickness.
K	The layer conductivity.
$P_{\text{PV,rated}}$	Rated power of each PV array.
η_{MMPT}	Efficiency of PV's DC/DC converter.
$\text{V}_{\text{cut}-\text{in}}$	Cut in wind speed.
$\text{V}_{\text{cut}-\text{off}}$	Cut out wind speed.
V	Wind speed.
V_{rated}	Nominal wind speed.
$P_{WG-\max}$	Maximum power of wind turbine.

Manuscript received June 06, 2013; revised November 25, 2013 and February 26, 2014; accepted April 20, 2014. Paper no. TSG-00431-2013.

S. M. Hakimi is with the K. N. Toosi University, Tehran 16315-1355, Iran (e-mail: Sm_hakimi@ieee.org).

S. M. Moghaddas-Tafreshi is with the Faculty of Engineering, Guilan University, Rasht 16315-1355, Iran (e-mail: Tafreshi@guilan.ac.ir).

Color versions of one or more of the figures in this paper are available online at http://ieeexplore.ieee.org.

Digital Object Identifier 10.1109/TSG.2014.2320962

P_{furl}	Power of wind turbine in cut out wind speed.
P_k^i	The best ever position of particle $i$at time k.
P_k^g	The global best position in the swarm at time k.
W_k	Inertia coefficient.
r_1 and r_2	Represent uniform random numbers between 0 and 1.
NPC_i	The net present cost of component i.
NPC_{loss}	The cost of loss of load and is calculated by.
NPC_{buy}	The cost of buying energy from distribution grid.
NPC_{sell}	The cost of selling energy to distribution grid.
$\text{N}_{\text{FC}}, \text{N}_{\text{WT}}$, N_{EL} and N_{PV}	Optimal size of fuel cell, wind turbine, electrolyzer and photovoltaic panel, respectively.

I. Introduction

TODAY in the majority of power systems operation techniques, the generation is controlled to supply the predicted network load. The direct control of loads are rare, except for the cases when insufficient generation is available on peak days, at which point the load may be reduced through demand response programs. The overall approach is that generation is controlled or dispatched to follow the load.

The load-following policy becomes more complicated as more renewable production is added to the grid [1]. In microgrids, intermittent renewable energy sources, such as wind and solar energies, are not dispatchable and predictable with an adequate assurance. Solar energy generation can alter rapidly due to passing clouds. Wind energy also has a different pattern every day with rapid daily changes. As a result, increase in the renewable generation capacity has to be accompanied with increase in conventional sources like peaking gas turbines [1]. With more and more intermittent renewable generation, it will become ever more complex for the residual dispatchable generation capacity to supply the required services and quick ramping to ensure that the generation follows the load. Fortunately, there is a novel opportunity brought forward by smart grid, which utilizes the direct control of loads [2]. As generation becomes less dispatchable in general, it can be somewhat compensated by making loads more dispatchable. Demand dispatch and demand response are alike in a way that demand response also involves turning loads on or off. Nevertheless, not like the demand response, which is used infrequently and typically for load shedding purposes during peak demand, demand dispatch is planned to be used enthusiastically at all times to be incorporated into services operating the grid [3]. It is called demand dispatch due to the fact that the loads are dispatched in real time, much as today's grid dispatches generation. Turning on a load or raising the demand on the grid creates similar results on the power balance of the grid as reducing the generation does. In a same way, turning off a load has the identical outcome as increasing the generation. Under demand dispatch, loads become generation- following [1].

Among all building services and electric appliances, the energy consumed by heating/cooling systems has the highest percentage [4]. Therefore, effective demand dispatch of the heating/cooling system can play an important role in creating the power balance.

In the present paper, the simulated smart microgrid contains wind turbines, solar panel, fuel cells, electrolyzer and smart heating/cooling systems. Heating/cooling systems are considered to be a flexible load which can be managed to follow the renewable energy generation as it allows increasing the penetration of renewable energy resources, thereby reducing the total cost of smart microgrid. This smart microgrid is connected to a distribution network. Consequently, the microgrid can sell its surplus power to the connected distribution network operator and buy shortage power from them whenever is needed.

The concept of the microgrid was first proposed by the Consortium for Electric Reliability Technology Solutions (CERTS) in America; it is a new type of distributed generation network structure with a wide range of development prospects [5]. Microgrids comprise low-voltage distribution systems with distributed energy sources, storage devices, and controllable loads, which operate either islanded or connected to the main power grid in a controlled, coordinated way. The authors in [6], [7] introduced the benefits of the microgrid, such as enhanced local reliability, reduced feeder losses, and local voltage support, providing increased efficiency using waste heat as combined heat and power, voltage sag correction, or providing uninterruptible power supply functions. The steady progress in the development of distributed power generation, such as microgrids and renewable energy technologies, is providing new opportunities for the utilization of energy resources.

Reference [8] shows that the intra-hour load balancing service supplied by HVAC loads meets the performance requirements and can become a main resource of income for load-serving entities where the two-way communication smart grid infrastructure enables direct load control over the HVAC loads. Reference [9] evaluates the performance of a centralized load controller designed to provide intra-hour load balancing services using air conditioning (A/C) units in their cooling modes. Reference [10] provides an optimization algorithm to manage a virtual power plant consisting of a large number of consumers with thermostatically controlled appliances. Reference [11] presents an intelligent residential air-conditioning (A/C) system controller that has smart grid functionality. Reference [12] investigates the demand response achieved by the smart energy management system in a smart home, and it aims to find the optimal temperature scheduling for air-conditioning according to the day-ahead electricity price and outdoor temperature forecasts.

Previous researches on comfort and energy management issues have mostly focused on large building environments with many occupants [13]–[16]. As detailed in the 2009 survey by Dounis and Caraiscos [17], these studies consider not only

heating and cooling systems but also other building design features such as window placements, window shading, mechanical ventilation systems, and lighting systems. Occupant comfort in these studies is typically a complex multi-faceted concept encompassing thermal comfort, visual comfort, and indoor air quality, in keeping with ASHRAE standards [18]. Various control methods are explored in these studies, including fuzzy controllers [19], fuzzy adaptive controllers [15], [20], and neural network controllers [21].

In recent years, the increasing interest in advanced metering infrastructure for households has encouraged researchers to focus more carefully on the energy usage choices for residential homeowners [22]. For example, a residential demand model, without consideration of price signals, proposed by Rogers *et al.* [23]. Guttromson *et al.* [24] and Chassin *et al.* [25] have focused on the modeling of price-responsive residential demands constrained by internal and external state conditions. The latter studies are anchored by an Olympic Peninsula pilot project [26]. However, residential energy demands in these studies are modeled by means of pre-specified behavioral rules rather than as solutions to residential optimization problems. More recent researches have set forth formulations of the residential A/C control problem as an optimization problem. However the current work has attempted to minimize the combination of thermal discomfort and energy usage under varying electricity prices [27]–[32].

The contributions of this paper are as follows:

1) In the assumed smart microgrid, the penetration of the intermittent renewable generation is high, and consequently the generation is less dispatchable. In this study, a new option is proposed to match load and generation by making loads more dispatchable. Previous studies can be extended to investigate the value of flexible loads in system with high renewable energy penetration.
2) In the previous works, peak shaving, displacing of controllable loads based consumption curves and electricity tariff have been proposed for load management. The present research has introduced a method to manage flexible loads using their consumption curves, generation side conditions and the welfare of consumers simultaneously.
3) Recent papers on heating/cooling systems management have only considered short time studies. To provide a more comprehensive study, this paper studies heating/cooling management over a longer time period. The economic and systematic impact of the proposed management methodology can be used in energy planning of a residential complex.

II. Active Controller

In the smart microgrid, the signal representing the surplus of power, Psurplus, is generated by a local controller and sent via a communication system to all end user active controllers. The surplus of power is the difference between renewable energy generation and load curve of smart microgrid. Ideally, the surplus power signal will be sent to the metering system of end users or Home Energy Management (HEM) systems, which then relay the information to the active controller(s) located inside the house. The surplus power signal is an indication of the availability of the renewable energy during a given time period. In addition to the surplus power signal, a rolling 24 hour average of the surplus power signal, $\mathrm{P}_{\mathrm{surplus,avg}}$, and a rolling 24 hour standard deviation of surplus power, $\sigma_{\mathrm{surplus,real}}$ are transmitted to the active controllers. The inclusion of the mentioned three signals allows for a comparison of the power signal over the past 24 hours. In order for an end use residential load to respond to the received signals, it is necessary to have an active controller on place.

This section examines the suggested solution for the active controller. An active controller operates by responding to a combination of internal set points and the external signal from the local control entity. Although the active controller can be connected to most end user loads, a residential heating/cooling system has been investigated in this paper.

A. Cooling Mode

The surplus power signal, $\mathrm{P}_{\mathrm{surplus}}$, and, $\mathrm{P}_{\mathrm{surplus,avg}}$, are transmitted to the controller as additional information which can be displayed for the end use on a HEM. When the surplus power signal is equal to the 24 hour average then the active controller will set the real temperature set point, $\mathrm{T}_{\mathrm{real}}$, to the $\mathrm{T}_{\mathrm{desired}}$. When the surplus power signal and the 24 hour average are not equal, $\mathrm{T}_{\mathrm{real}}$ will be shifted away from the $\mathrm{T}_{\mathrm{desired}}$. If the surplus power signal is lower than the 24 hour average, the controller will move the real cooling set point, $\mathrm{T}_{\mathrm{real}}$, higher than the desired temperature set point, $\mathrm{T}_{\mathrm{desired}}$, The maximum allowable temperature will not exceed $\mathrm{T}_{\mathrm{max}}$. On the other hand, when the surplus power signal is higher than the 24 hour average, the controller will reduce the real cooling set point lower than the desired temperature, with the minimum value of $\mathrm{T}_{\mathrm{min}}$. The difference between the desired and real set point is given by $\Delta\mathrm{T}$. Any positive value of $\Delta\mathrm{T}$ $(\Delta\mathrm{T} > 0)$ indicates that the real set point is higher than the desired set point. In effect the cooling system allows the temperature set point to increase as the surplus power signal is lower than the average value. Conversely, any negative value of $\Delta\mathrm{T}$ $(\Delta\mathrm{T} < 0)$ indicates that the controller has moved the real set point lower than the desired set point. In effect, the cooling system preemptively continues to cool down the temperature because of the surplus power signal is higher than average value.

While $\mathrm{P}_{\mathrm{surplus}}$ and $\mathrm{P}_{\mathrm{surplus,avg}}$ are used for conceptual and informational purposes, the active controller will operate based on $\sigma_{\mathrm{surplus,real}}$. Since $\sigma_{\mathrm{surplus,real}}$ is a function of the current surplus power and the average surplus power for the past 24 hours, $\mathrm{P}_{\mathrm{surplus}}$ and $\mathrm{P}_{\mathrm{surplus,avg}}$ are operationally redundant values. A graphical representation of the correlation between $\sigma_{\mathrm{surplus,real}}$ and the temperature set points can be seen in Fig. 1.

From Fig. 1 it can be seen that R_{low} and R_{high} can have different values, indicating different end use preferences for heating and cooling response. For example, a customer may be willing to have their house temperature increased above the desired cooling set point but they are reluctant to allow temperature to decrease below the cooling set point. Additionally, T_{min} and T_{max} do not need to be symmetric around the desired temperature set point. The real temperature set point of the active controller is determined by (1) and is subject to constraints of

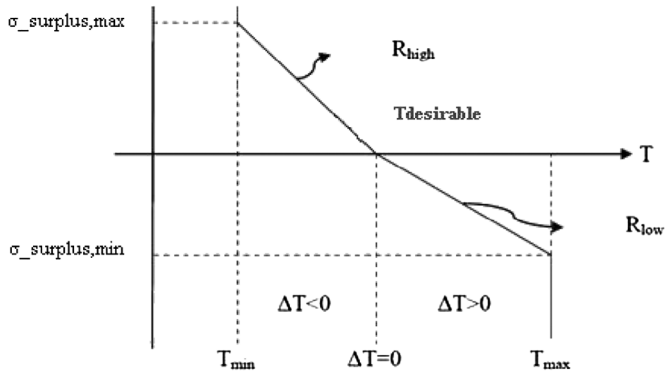

Fig. 1. Active controller for a cooling system.

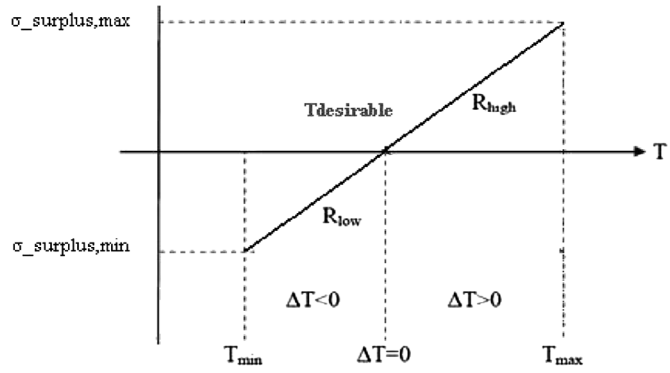

Fig. 2. Active controller for a heating system.

(2). $R_{\text{low}}, R_{\text{high}}$, 24 hour average surplus power and $\sigma_{\text{surplus,real}}$ are determined by ((3)–(6)), respectively.

$$T_{\text{real}} = T_{\text{desirable}} + \Delta T \tag{1}$$

$$T_{\min} - T_{\text{desirable}} \leq \Delta T \leq T_{\max} - T_{\text{desirable}} \tag{2}$$

$$R_{\text{high}} = \frac{\sigma_{\text{surplus,max}}}{T_{\max} - T_{\text{desirable}}} \; if \; \sigma_{\text{surplus,real}} > 0 \tag{3}$$

$$R_{\text{low}} = \frac{\sigma_{\text{surplus,min}}}{T_{\max} - T_{\text{desirable}}} \; if \; \sigma_{\text{surplus,real}} < 0 \tag{4}$$

$$\sigma_{\text{surplus,real}} = \frac{P_{\text{surplus}} - O_{\text{surplus,avg}}}{P_{\text{surplus,avg}}} \tag{5}$$

$$P_{\text{surplus,avg}} = \frac{\sum_{i=1}^{24} P_{\text{surplus},i}}{24}. \tag{6}$$

In order to determine the real value of ΔT at any given time, initially it is necessary to determine if the present surplus power signal is higher or lower than the 24 hour average. This will be known by the sign of $\sigma_{\text{surplus,real}}$ (5). For a residential cooling system a positive value indicates that the current surplus power is lower than the 24 hour average and a negative sign indicates that it higher. Assuming a zero value $\sigma_{\text{surplus,real}}$ does not generate any ΔT, the value of ΔT for a cooling system where $\sigma_{\text{surplus,real}} > 0$ is given by (7) and $\sigma_{\text{surplus,real}} < 0$ is given by (8).

$$\Delta T = \frac{\sigma_{\text{surplus,real}}}{R_{\text{high}}} \quad \sigma_{\text{surplus,real}} > 0 \tag{7}$$

$$\Delta T = \frac{\sigma_{\text{surplus,real}}}{R_{\text{low}}} \quad \sigma_{\text{surplus,real}} < 0. \tag{8}$$

Combining (1), (7), and (8) yield (9) and (10) which are still subject to the constraint determined by (2). When $\text{P}_{\text{surplus}} > \text{P}_{\text{surplus,avg}}$, yields a $\sigma_{\text{surplus,real}_1} > 0$, the real temperature set point is given by (9) and when $\text{P}_{\text{surplus}} < \text{P}_{\text{surplus,avg}}$, yields a $\sigma_{\text{surplus,real}} < 0$, the real temperature set point is given by (10).

$$T_{\text{real}} = T_{\text{desirable}} + \frac{\sigma_{\text{surplus,real}}}{R_{\text{high}}} \quad \sigma_{\text{surplus,real}} > 0 \tag{9}$$

$$T_{\text{real}} = T_{\text{desirable}} + \frac{\sigma_{\text{surplus,real}}}{R_{\text{loss}}} \quad \sigma_{\text{surplus,real}} < 0. \tag{10}$$

A key observation from Fig. 1 and (9) and (10) is that there are no absolute surplus power values or temperature set points. The active controller operates to adjust the real temperature set point based on a standard deviation of the surplus power signal and internal set points, which indicate the end users willingness to have their cooling set point adjusted from the desired value. Additionally, absolute temperature set points would mean that the controller would not have the flexibility to provide demand response when end users changed their desired temperature set points. The flexibility of being able to operate in different surplus power levels is essential for a device which is designed for residential application in smart microgrid with high penetration of the renewable energy.

B. Heating Mode

If the surplus power signal is higher than the 24 hour average, the controller will tend to move the real heating set point higher than the desired temperature set point, but it will not exceed $\text{T}_{\max}$. Conversely, when the surplus power signal is lower than the 24 hour average, the controller will tend to move the real heating set point lower than the desired temperature, but it will not exceed $\text{T}_{\min}$. For an active controller operating on a heating system, $\Delta\text{T} > 0$ indicates that the real set point is higher than the desired set point. In effect, the heating system is allowing the temperature set point to increase because of the surplus power signal being higher than average. Conversely, $\Delta\text{T} < 0$ indicates that the controller has moved the real set point lower than the desired set point. In effect, the heating system is preemptively heating because of the surplus power signal being lower than average.

A graphical representation of the correlation between $\sigma_{\text{surplus,real}}$ and the temperature set points can be seen in Fig. 2. The real temperature set point of the active controller is determined by (1) and subject to the constraints of (2).

In heating mode R_{high} and R_{low} are calculated as follows:

$$R_{\text{high}} = \frac{\sigma_{\text{surplus,max}}}{T_{\max} - T_{\text{desirable}}} \quad if \; \sigma_{\text{surplus,real}} > 0 \tag{11}$$

$$R_{\text{low}} = \frac{\sigma_{\text{surplus,min}}}{T_{\min} - T_{\text{desirable}}} \quad if \; \sigma_{\text{surplus,real}} < 0. \tag{12}$$

For a residential heating system, a positive value indicates that the current surplus power is higher than the 24 hour average, and a negative sign indicates that it lower. Then, assuming that a $\sigma_{\text{surplus,real}}$ of 0 generates a ΔT of 0, the value of ΔT for a heating system where $\sigma_{\text{surplus,real}} > 0$ is given by (7), and $\sigma_{\text{surplus,real}} < 0$ is given by (8).

When $\mathrm{P_{surplus}} > \mathrm{P_{surplus,avg}}$, yielding a $\sigma_{\mathrm{surplus,real}} > 0$, the real temperature set point is given by (9), and when $\mathrm{P_{surplus}} < \mathrm{P_{surplus,avg}}$, yielding a $\sigma_{\mathrm{surplus,real}} < 0$, the real temperature set point is given by (10).

III. Determine Power Consumption of Heating/Cooling System

According to the proposed method in previous section, the indoor temperature variation is calculated as follows:

$$\Delta \mathrm{T}'_{\mathrm{i}} = \mathrm{T}_{\mathrm{real_i}} - \mathrm{T}_{\mathrm{real_{i-1}}} \tag{13}$$

where $\mathrm{T}_{\mathrm{real1}}$ is the actual temperature at time i, and $\mathrm{T}_{\mathrm{real_{i-1}}}$ is the actual temperature at time i-1. The heating/cooling system should supply the temperature variation of $\Delta \mathrm{T}'_{\mathrm{i}}$.

In order to satisfy the deviation of the pointed temperature, (14) should be established.

$$\mathrm{Q_{AC_i}} - \mathrm{Q_{loss}} = -\mathrm{m}.\mathrm{c_{air}}.\Delta \mathrm{T}'_{\mathrm{i}} \tag{14}$$

$\mathrm{Q_{loss}}$ is the thermal loss between the indoor and outdoor environment through the wall, window, and ceiling surfaces and the sum of internal loads.

Equation (14) can be rewritten as follows:

$$Q_{AC\,i} - Q_{\mathrm{loss}\,i} = -\rho_{\mathrm{air}}.V_{\mathrm{room}}.c_{\mathrm{air}}\Delta T'_i \tag{15}$$

The heating/cooling efficiency is often rated by the Seasonal Energy Efficiency Ratio (SEER). The SEER rating of a unit is the heating/cooling output during a typical cooling (heating) season divided by the total electric energy input during the same period. The higher the unit's SEER rating, the more energy efficient it is [32].

Equation (15) can be rewritten as follows:

$$P_{CA\,i} \times t \times SEER - Q_{\mathrm{loss}\,i} = -\rho_{\mathrm{air}}.V_{\mathrm{room}}.c_{\mathrm{air}}.\Delta T'_i \tag{16}$$

$$P_{AC\,\min} \le P_{AC\,i} \le P_{AC\,\max} \tag{17}$$

where $P_{AC\,i}$ is the power consumption of the heating/cooling system at time i, and t is time interval (one hour in this study).

1) Q_{loss} for Cooling System: The following parameters have to be considered for evaluating the the cooling load [18]:

1) Solar and transmission heat gain through the exterior walls, roofs and glasses.
2) Heat gain due to the ventilation or infiltration.
3) Heat gain through interior partitions.
4) Internal load, including heat rejection from equipment, lighting and occupants.

Cooling load is the sum of radiation, conduction, convection, and internal loads. Radiation is related to the sunshine and the sun energy absorbed by the building construction. Conduction load is calculated as heating but by cooling data. The convection load contains the sensible load as heating and the latent load of the air infiltrated by the formula below [18].

$$Q_{\mathrm{Latent}} = CMH \times 0.82 \times \Delta W \tag{18}$$

where Q_{Latent} latent load (W), CMH (Cubic Meter per Hour) is infiltration air flow (m3/hour), 0.82 is the latent heat factor (at sea level), and ΔW is the air specific humidity difference between inside and outside the space (gr/kg of dry air).

Internal loads include, heat dissipation of equipments, peoples, and lights.

Conduction heating load is calculated by (19) [18]:

$$Q_{\mathrm{Conduction}} = U \times A \times \Delta T \tag{19}$$

where $\mathrm{Q_{Conduction}}$ is the conduction heating load (W), U is the heat transmission coefficient (W/m2C), A is the Construction layer area (m2), and $\Delta \mathrm{T}$ is the air temperature difference between outside and inside the space ($^{\circ}\mathrm{C}$).

The heat transmission coefficient (U) can be calculated as follows:

$$\mathrm{U} = \frac{1}{\sum \mathrm{R_i}} \tag{20}$$

$$\mathrm{R_i} = \frac{\mathrm{x_i}}{\mathrm{k_i}} \tag{21}$$

where R is the thermal resistance of structure layers (m2c/w), x is the layer thickness (mm), and k is the layer conductivity (W.mm/m2c).

Convection heating load can be calculated as follows [18]:

$$\mathrm{Q_{Converction}} = 0.335 \times \mathrm{CHM} \times \Delta \mathrm{T} \tag{22}$$

where $\mathrm{Q_{Convection}}$ is convection heating load (W), 0.335 is sensible heat factor (at see level), CMH is the air flow infiltration rate (m3/hour), and $\Delta \mathrm{T}$ is the air temperature difference between outside and inside the space ($^{\circ}\mathrm{C}$).

Therefore for cooling system, $\mathrm{Q_{loss}}$ can be calculated as follows:

$$\mathrm{Q_{loss}} = \mathrm{Q_{Latent}} + \mathrm{Q_{Conduction}} + \mathrm{Q_{Convection}} \tag{23}$$

2) $\mathrm{Q_{loss}}$ for Heating System: Heating load estimation involves the following [18]:

(a) Heat loss through exterior walls, roofs, glasses, doors, and floor.
(b) Ventilation or infiltration loss.

Heating load is the sum of conduction and convection heat transmission rates. Conduction heating load and convection heating load are calculated by (19) and (22), respectively. Therefore for heating system, $\mathrm{Q_{loss}}$ can be calculated as follows:

$$\mathrm{Q_{loss}} = \mathrm{Q_{Conduction}} + \mathrm{Q_{Convection}} \tag{24}$$

Fig. 3 shows a flowchart of the proposed method.

IV. Renewable Energy and Storage Modeling

A. Photovoltaic Array

The output power of each PV array, with respect to the solar radiation power, can be calculated through (25).

$$P_{PV} = \frac{G}{1000} \times P_{\mathrm{PV,rated}} \times \eta_{\mathrm{MMPT}} \tag{25}$$

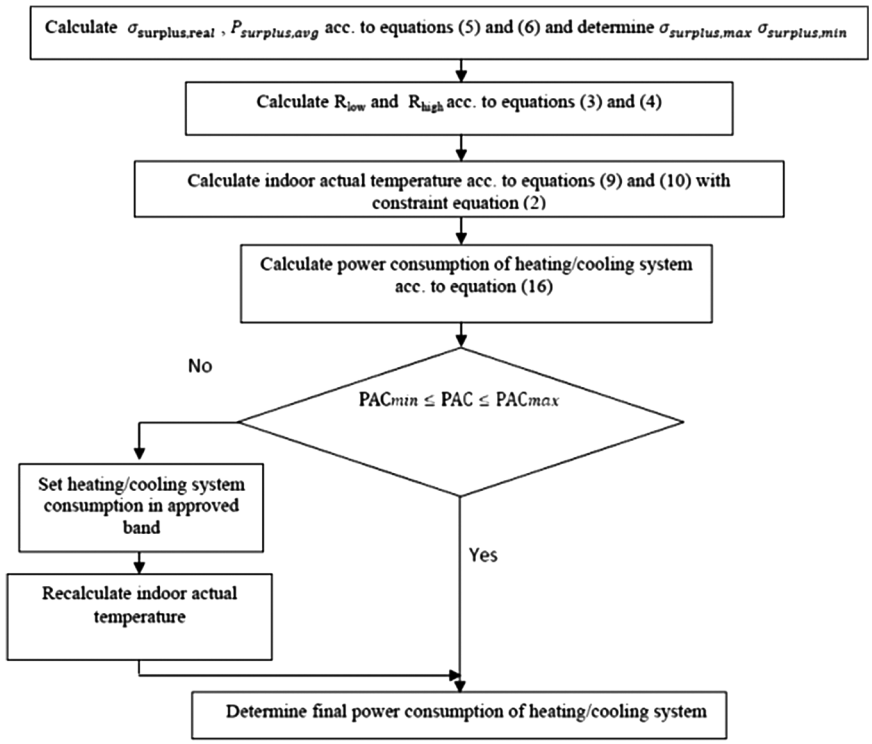

Fig. 3. Flowchart of proposed method.

where, G is perpendicular radiation at array's surface (W/m2), $P_{\mathrm{PV,rated}}$ is rated power of each PV array at G = 1000 W/m2, and η_{MMPT} is the efficiency of PV's DC/DC converter and Maximum Power Point Tracking System (MPPT). PV systems are usually equipped with MPPT systems to maximize the power output. Therefore, it is reasonable to believe that the PV array working states stay around the maximum power point [33].

B. Wind Turbine Generator

The power curve versus wind speed is approximated by (26), shown at the bottom of the next page.

Hydrogen Tank: By adding output powers of wind turbine and photovoltaic, injected power to the DC bus, generated by renewable sources, is calculated as:

$$P_{ren}\left(n_{WG}^{\mathrm{fail}}, n_{PV}^{\mathrm{fail}}\right) = \left(N_{WG} - n_{WG}^{\mathrm{fail}}\right) \times P_{WG} + \left(N_{PV} - n_{PV}^{\mathrm{fail}}\right) \times P_{PV} \quad (27)$$

where N_{WG}, N_{PV}, n_{WG}^{fail}, and n_{PV}^{fail} are numbers of installed and failed WG turbines and PV arrays, respectively. The availability and unavailability of system components significantly affect reliability of the system. Components may be unavailable because of scheduled (like maintenance program) or forced (like component failure) outages [34]. Generated power by renewable sources flows through two streams. First stream goes to the inverter to supply the load $(\mathrm{P}_{\mathrm{ren_{inv}}})$, and the second one delivers the surplus power to the electrolyzer for hydrogen production $(\mathrm{P}_{\mathrm{ren\_el}})$.

$$P_{\mathrm{el-tank}} = P_{\mathrm{ren-el}} \times \eta_{el} \quad (28)$$

$$E_{\mathrm{tank}}(t) = E_{\mathrm{tank}}(t-1) + P_{\mathrm{el-tank}}(t) \times \Delta t - P_{tank-FC}(t) \times \Delta t \times \eta_{\mathrm{storage}} \quad (29)$$

where η_{el} is electrolyzer's efficiency which is assumed to be constant for whole operational range [35]. $P_{tank-FC}$ is the transferred power from the hydrogen tank to the FC. Storage efficiency $(\eta_{\mathrm{storage}})$ may present losses resulted from leakage or pumping, and it is assumed to be equal to 95% for all working states [36]. The mass of stored hydrogen, at any time step t, is calculated as follows:

$$m_{\mathrm{storage}}(t) = \frac{E_{\mathrm{storage}}(t)}{\mathrm{HHV}_{H_2}} \quad (30)$$

where the higher heating value (HHV) of hydrogen is equal to 39.7 kWh/kg [37].

$$\begin{cases} 0 & V < V_{\mathrm{cut-in}}, V > V_{\mathrm{cut-off}} \\ P_{WG-\max} \times \left((V - V_{\mathrm{cut-in}})/(V_{\mathrm{rated}} - V_{\mathrm{cut-in}})\right)^3 & V_{\mathrm{cut-in}} \le V < V_{\mathrm{rated}} \\ P_{WG-\max} \times \frac{P_{furl} - P_{\mathrm{rated}}}{V_{\mathrm{cut-off}} - V_{\mathrm{rated}}} \times (V - V_{\mathrm{rated}}) & V_{\mathrm{rated}} \le V \le V_{\mathrm{cut-off}} \end{cases} \quad (26)$$

C. Fuel Cell

Fuel cell output power can be defined as a function of its input and efficiency (η_{FC}), which is assumed to be constant (here, 50%) [35]

$$P_{\mathrm{FC-inv}} = P_{\mathrm{tank-FC}} \times \eta_{\mathrm{FC}} \tag{31}$$

V. Particle Swarm Optimization

Particle swarm optimization was introduced in 1995 by Kennedy and Eberhart [38]. Although several modifications to the original algorithm have been made to improve its performance [39]–[43] and adapt it to specific types of problems [44]–[46], a parallel version has not been previously implemented. The following is a brief introduction to the operation of the PSO algorithm. Consider a swarm of p particles, with each particle' s position representing a possible solution point in the design problem space D. For each particle i, Kennedy and Eberhart proposed that its position $X^i$is updated in the following manner:

$$X_{k+1}^i = X_k^i + V_{k+1}^i \tag{32}$$

with a pseudo-velocity V_{k+1}^i calculated as follows:

$$V_{k+1}^i = W_k V_k^i + C_1 r_1 \left(P_k^i - X_k^i\right) + C_2 r_2 \left(P_k^g - X_k^i\right). \tag{33}$$

Here, subscript k indicates a pseudo-time increment, and W_k is the inertia coefficient which is employed to manipulate the impact of the previous history of velocities on the current velocity. To allow the product $C_1 r_1$ or $C_2 r_2$ to have a mean of 1, Kennedy and Eberhart proposed that the cognitive and social scaling parameters C_1 and C_2 are selected such that $C_1 = C_2 = 2$. Fig. 4 depicts the optimization flowchart of PSO algorithm.

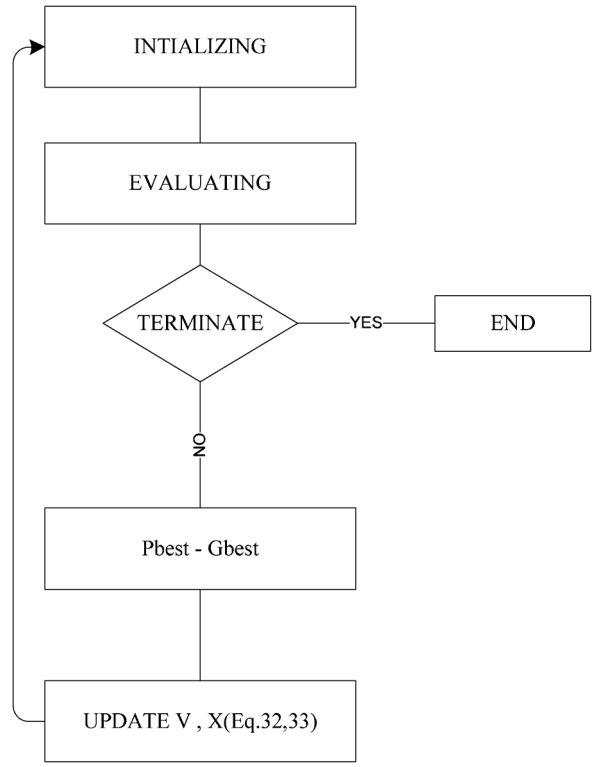

Fig. 4. Optimization flowchart of PSO algorithm.

VI. Objective Function

The objective function of this paper is

$$J = \min_X \left\{ \sum_i NPC_i + NPC_{\mathrm{loss}} + NPC_{\mathrm{buy}} - NPC_{\mathrm{sell}} \right\} \tag{34}$$

$$NPC_i = N_i \times \left(CC_i + RC_i \times K(ir, L_i, y_i) + O\&M_i \times \frac{1}{CRF(ir, R)}\right) \tag{35}$$

where N is the number (unit) or capacity (kW or kg), CC is capital cost ($/unit), RC is cost of replacement ($/unit), and O&M is annual operation and maintenance cost ($/unit-yr) of the components:

$$ir = \frac{(ir_{nominal} - f)}{(1+f)} \tag{36}$$

where ir is the real interest rate (here 6%) which is a function of nominal interest rate $(ir_{nominal})$ and annual inflation rate (f).

$$K(ir, L_i, y_i) = \sum_{n=1}^{y_i} \frac{1}{(1+ir)^{n \times L_i}} \tag{37}$$

$$CRF(ir, R) = \frac{ir(1+ir)^R}{(1+ir)^R - 1}. \tag{38}$$

R is the useful lifetime of the project (here 20 years). L and y are useful lifetime and number of replacement of the component during useful lifetime of the project, respectively.

NPC_{loss} is calculated by

$$NPC_{\mathrm{loss}} = LOEE \times C_{\mathrm{loss}} \times \frac{1}{CRF(ir, R)} \tag{39}$$

$$LOEE = \sum_{t=1}^{8760} E\left[LOE(t)\right] \tag{40}$$

where $E[LOE(t)]$ is the expected value of loss of energy or energy not supplied, at time step t defined by

$$E[LOE] = \sum_{s \in S} Q_s \times P_s. \tag{41}$$

Here, Q_s is the amount of loss of energy (kWh) when system encounters state s, and P_s is the probability that system encounters in state s.

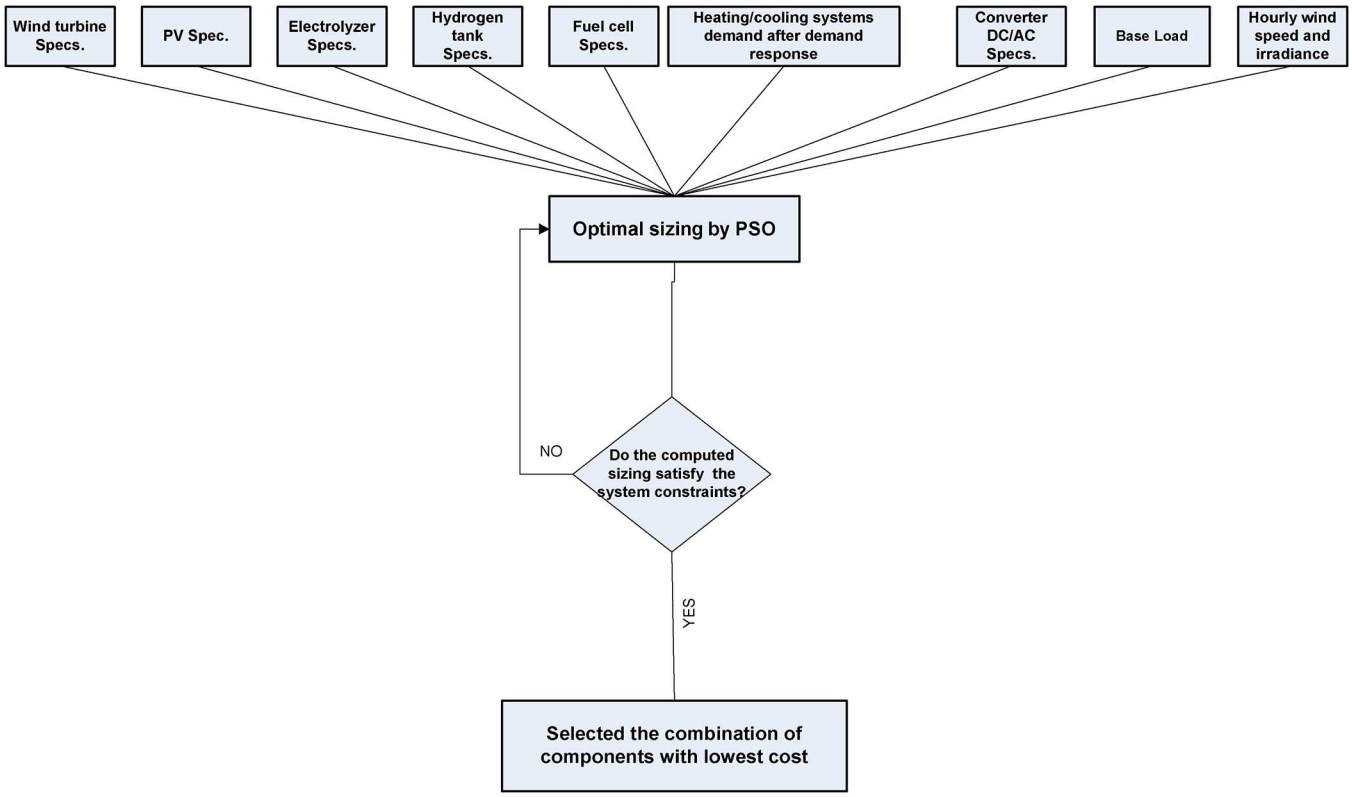

Fig. 5. Flowchart of the proposed optimization methodology.

NPC_{buy} and NPC_{sell} are described by the following equations:

$$NPC_{\text{buy}} = \sum_{t=1}^{8760} P_{\text{buy}}(t) \times C_{\text{buy}}(t) \times \frac{1}{CRF(ir,R)} \tag{42}$$

$$NPC_{\text{sell}} = \sum_{t=1}^{8760} P_{\text{sell}}(t) \times C_{\text{sell}}(t) \times \frac{1}{CRF(ir,R)}. \tag{43}$$

$P_{\text{buy}}(t)$ *is the* power which purchased from the grid, and $P_{\text{sell}}(t)$ is the power which sold to grid. $C_{\text{buy}}(t)$ and $C_{\text{sell}}(t)$ are the prices of buying and selling power, respectively.

The optimization problem is subject to the following constraints:

$$ELF = \frac{1}{H} \sum_{t=1}^{H} \frac{Q(t)}{D(t)} \tag{44}$$

where H is the number of time steps in which system's reliability is evaluated (here, H = 8760). The equivalent load factor (ELF) is the ratio of the effective forced outage hours to the total number of hours. In fact, it contains information about both the numbers and magnitudes of the outages [47]. Therefore, ELF is chosen as the main reliability index of this study:

$$E[ELF] \leq ELF_{\max} \tag{45}$$

$$0 \leq N_i \leq N_{\max} \tag{46}$$

$$E_{\text{tank}}(0) \leq E_{\text{tank}}(8760) \tag{47}$$

$$0 \leq P_{\text{buy}}(t) \leq P_{buy(\max)} \tag{48}$$

$$0 \leq P_{\text{sell}}(t) \leq P_{sell(\max)}. \tag{49}$$

VII. Simulation Result

In this study, Ekbatan residential area (Tehran, Iran) has been selected as a case study. The peak load of the considered smart microgrid, phase A of Ekbatan complex, is 500 kW (the overall load curve without heating and cooling load), and the number of houses are 200. Ekbatan has three separate sets of buildings called respectively phase A, B, and C. Each phase has isolated buildings called a block. The architecture in the first and the third phase is similar and different from the phase B. All of these phases contain 1, 2, 3, or 4-bedroom apartments occupying an area within the range of 50 m^2 to 240 m^2.The size of each wind turbine and other units (Photovoltaic, Fuel cell, electrolyzer, and hydrogen tank) are considered 7.5 kW and 1 kW, respectively. Fig. 5 shows the system flowchart.

This paper determines the optimal size of units for the smart microgrid considering intelligent management of heating/cooling loads. Air conditioning system has been used in order to provide heating/cooling inside the houses. Also, the requirement of heat water is supplied by the output heat water generated by fuel cell and municipal waste. If the mentioned sources are not able to supply sufficient heat water, the natural gas will be purchased as a replacement. This paper intends to investigate the effect of heating and cooling management on optimal size of smart microgrid units, the reliability of loads, the amount of purchased natural gas from utility, and the total cost of the smart microgrid. The management of heating and cooling loads is performed by considering renewable energy production including wind and solar resources, smart microgrid

TABLE I
THE ELECTRICAL ENERGY TARIFFS OF RESIDENTIAL CONSUMPTION

	Middle load	Peak load	Off-peak load
Hour	7-19	19-23	23-7
$/kWh(the power more than 30kW)	0.034	0.068	0.017
$/kWh(the power less than 30kW)	0.044	0.088	0.022

load curves, the outside temperature, and the desired inside temperature of the consumers.

In order to achieve optimal sizing of smart microgrid units, the following parameters should be determined as the program inputs:

- Characteristic of generation units of smart microgrid, i.e. wind and solar resources.
- Characteristic of energy storage, i.e. fuel cell, electrolyzer, and hydrogen tank.
- Hourly wind speed and solar irradiation in order to specify the production of wind and solar units.
- Outside temperature.
- Desired temperature, maximum and minimum acceptable temperature.
- The price of energy purchased and bought from and to distribution grid.
- The price of natural gas.
- Hourly load curve.
- The minimum and maximum power consumptions of a typical air conditioner.
- The required parameters of optimization algorithm, i.e. Particle Swarm Optimization (PSO).
- The features of mentioned buildings such as wall material, windows, and etc.

The insertion of above-mentioned parameters and running the program will result in the following output:

- The optimal size of smart microgrid elements.
- The rate of energy generated by wind and solar resources and fuel cell.
- The rate of hydrogen storage in related tank.
- The rate and the cost of energy transfer between the considered smart microgrid and distribution grid.
- The rate of heating/cooling system power consumption.
- The hourly real inside temperature.
- The not-supply load, load reliability, and penalty of not-supply load.
- The optimal cost of the smart microgrid.

In the performed simulations, a transformer with a capacity of 100 kVA and 90% efficiency provides a bidirectional connection between the smart microgrid and the distribution grid. The considered electrical energy tariffs within this study refer to the residential subscriber in the range of consumption more than 30 kW and less than 30 kW in Iran. The tariffs are shown in Table I.

TABLE II
OPTIMAL COST AND SIZE OF EACH UNIT IN SMART MICROGRID WITHOUT MANAGING THE HEATING/COOLING SYSTEMS

Cost($)	Trans. (KVA)	N_{FC}	Hydrogen tank	N_{EL}	N_{WT}	N_{PV}
1.96361×10^7	55	521	4398	874	201	597

TABLE III
THE AMOUNT AND COST OF BUYING AND SELLING ENERGY, THE AMOUNT AND COST OF BUYING NATURAL GAS, INTERRUPTED LOADS AND PENALTY FOR THEM WITHOUT MANAGING THE HEATING/COOLING SYSTEMS

Cost of buying natural gas ($)	Buying natural gas(m3)	ELF	Penalty for Interrupted loads ($)	Interrupted loads (kWh)
2.064×10^3	2.103×10^4	0.00253	8.4508×10^5	15.3702×10^3

Cost of selling energy($)	Selling energy (kWh)	Cost of buying energy($)	Buying energy (kWh)
1.052×10^5	1.0716×10^5	2.194×10^4	2.234×10^4

Regarding the price of produced electricity in non-governmental sections out of new energies resources and with regard to the positive environmental aspects and economies by lack of consumption of fossil energy resources and in order to encourage any investment in this type of production, it is applicable for one kwh for peak & normal hours at least 0.13$ and for low-load hours at least 0.09$ (Maximum 4 hours per day/night) in production place [48].

In order to implement the heating/cooling system load control method, the area of houses (where heating/cooling system is installed) is considered with dimensions of 10 m $\times$ 16 m. It is assumed that the thermal interchange is accrued with the side walls, i.e. $(50\ \mathrm{m}^2 + 50\ \mathrm{m}^2 + 28\ \mathrm{m}^2 + 28\ \mathrm{m}^2)$. 20% of the front and back side walls are being made of double glazed windows with 1 cm thicknesses and 5% of them of fiber glazed windows. Based on the calculation, the k factor of window equals to 0.05 (w/m.k), and walls thickness is 30 cm.

The optimal numbers of smart microgrid units before managing the power consumption of heating and cooling system are demonstrated in Table II. The optimal amount and cost of purchased power from the distribution grid, the optimal amount and cost of sold power to distribution grid, the optimal cost of the smart microgrid, interrupted loads, penalty for interrupted loads, the optimal amount and cost of purchased natural gas and smart microgrid reliability are depicted in Table III.

This section investigates the effect of management of heating and cooling loads on optimal sizing of smart microgrid units. The proposed control methodology requires the following parameters to be determined:

- The desired temperature in hot season, i.e. summer: 23°C
- The desired temperature in cold season, i.e. winter: 21°C
- The minimum and maximum temperature in summer: 19–26°C
- The minimum and maximum temperature in winter: 18–22°C
- Maximum power consumption of each heating/cooling system is assumed to be 1.7 kW.

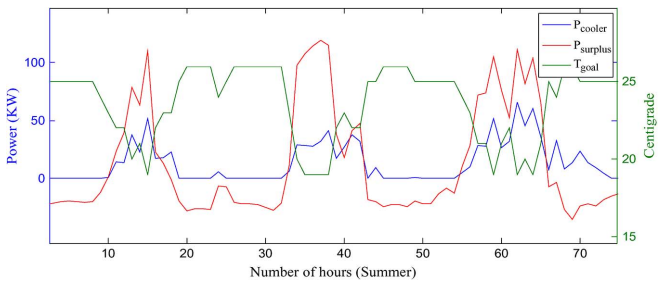

Fig. 6. The surplus power of renewable energy sources, adjusted temperature and the cooling system power.

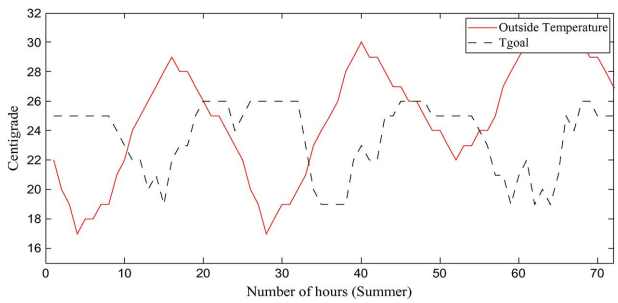

Fig. 7. The actual inside temperature of the house and the outside temperature in summer.

Based on these assumptions, the above mentioned control method is applied in order to model and manage the heating and cooling system.

Fig. 6 shows the smart microgrid's extra power for three days of a hot season, adjusted temperature inside the house (T_{goal}) and managed (controlled) power of the cooling system on a same time scale. As can be seen in Fig. 6, during hours which we have extra power the house temperature is adjusted to be less than the desired temperature (within the constraints). This will change the behaviour (consumption) of the cooling system to match the available the extra power. Also, during the hours when the surplus of power is negative the temperature is tuned for a value higher than desired one, to minimize the consumption of the cooling system. Fig. 7 shows the actual inside temperature of the house (T_{goal}) and the outside temperature in summer. The inside temperature of the house will be changed according to the surplus power, i.e. when surplus power is low, the inside temperature will be set to an upper point and vice versa.

In the proposed method, using the active controller, consumers choose a temperature as the desired temperature, and then, the active controller will calculate a temperature for the internal space based on the desired temperature and the mentioned extra power. Finally, the controller set the power consumption of heating/cooling system according to the outside temperature in order to reach the calculated temperature which is nominated with actual temperature. This temperature should satisfy the following conditions,

- To decrease the power consumption heating/cooling system while the surplus power is low.
- Not to interfere with the thermal comforts of the consumers.

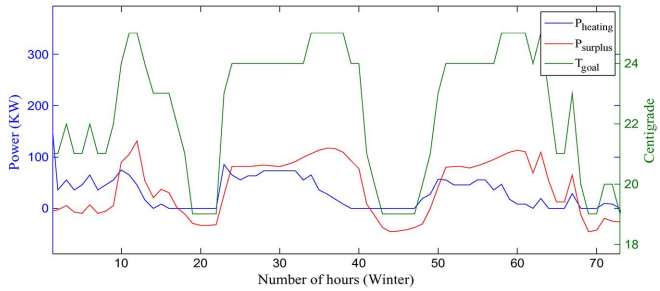

Fig. 8. The surplus power of renewable energy sources and the heating system power.

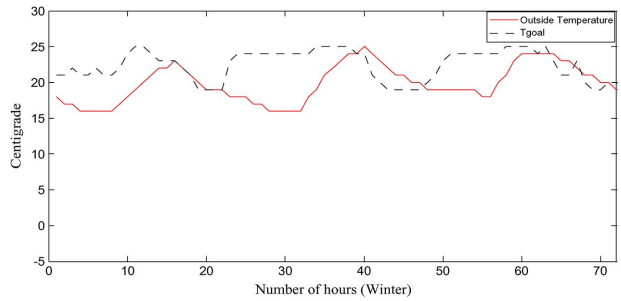

Fig. 9. The actual inside temperature of the house and the outside temperature in winter.

TABLE IV
OPTIMAL COST AND SIZE OF EACH UNIT IN SMART MICROGRID WITH MANAGING THE POWER CONSUMPTION OF HEATING AND COOLING SYSTEM

Cost($)	Trans. (KVA)	N_{FC}	Hydrogen tank	N_{EL}	N_{WT}	N_{PV}
1.8009×10^7	90	521	4833	681	162	342

In other words, the controller decides on heating or cooling the inside with regards to the thermal comfort of consumers and the surplus power.

The proposed method also is applied to power consumption of heating systems. Fig. 8 shows the smart microgrid's extra power for three days of a cold season, adjusted temperature inside the house (T_{goal}) and managed (controlled) power of the heating system on a same time scale. In this figure, during hours when the surplus of power is positive the home temperature is adjusted higher than the desired value in order to match the heating system consumption with the extra available power. On the other hand, during the hours when the surplus of power is negative, the temperature will be lower than the desired to reduce the cooling system consumption and consequently better matching the consumed power with the available extra power.

Fig. 9 shows the actual inside temperature (T_{goal}) of the house and the outside temperature in winter.

The optimal numbers of smart microgrid units after managing the power consumption of heating and cooling systems are demonstrated in Table IV. The optimal amount of purchased power from distribution grid, the optimal amount of sold power to distribution grid and the not-supply loads, considering related costs and smart microgrid reliability are depicted in Table V.

By comparing n Tables II and IV it can be noted that utilizing the proposed method to manage the power consumption of heating and cooling system will decrease the size of renewable energy generators (wind and solar) and increase the amount of stored hydrogen in the hydrogen tank. Also the comparison

TABLE V
THE AMOUNT AND COST OF BUYING AND SELLING ENERGY, THE AMOUNT AND COST OF BUYING NATURAL GAS, INTERRUPTED LOADS AND PENALTY FOR THEM WITH MANAGING THE HEATING/COOLING SYSTEMS

Cost of buying natural gas ($)	Buying natural gas(m3)	ELF	Penalty for Interrupted loads ($)	Interrupted loads (kWh)
847.43	8631	0.000153	48765	887

Cost of selling energy($)	Selling energy (kWh)	Cost of buying energy($)	Buying energy (kWh)
1.497×10^5	1.525×10^5	7.374×10^3	7.51×10^3

of Tables III and V illustrates that the proposed method will result in reduction of the purchased power from distributed grid, thereby increasing the power sold to the distributed grid as well as decreasing non-supply loads and purchased gas from the utility.

To verify the presented cooling/heating system management method, the correlation of cooling system loads prior to and after application of the load management method with the power surplus curve has been investigated. The correlation values are as follows:

$$\mathrm{Correlation}(\mathrm{Psurplus}, \mathrm{Pcooler}_{Unmannaged}) = 0.49 \tag{50}$$

$$\mathrm{Correlation}(\mathrm{Psurplus}, \mathrm{Pcooler}_{Mannaged}) = 0.78 \tag{51}$$

The resulted values show that employing the proposed load management method will increase the correlation between cooling system loads and surplus power of renewable energy sources. In other words, the rate of change of cooling system power usage gets closer to the rate of change of the surplus energy produced by renewable sources. This in turn creates the capacity for higher renewable energy penetration.

The total load in consists of two parts:

1) The base load *Pbase(i)* represents the all electricity loads within a smart microgrid except cooling and heating loads.
2) *Pcooling(i)* and *Pheating(i)* represent the load of cooling and heating systems respectively.

The measurement interval is recorded hourly and denoted by i. It is assumed that the base load *Pbase(i)* remains constant during the measured interval i.

$$\mathrm{Pload}_{Old}(\mathrm{i}) = \mathrm{Pbase(i)} + \mathrm{Pcooling}_{Unmannaged}(\mathrm{i}) + \mathrm{Pheating}_{Unmannaged}(\mathrm{i}) \tag{52}$$

$$\mathrm{Pload}_{New}(\mathrm{i}) = \mathrm{Pbase(i)} + \mathrm{Pcooling}_{Mannaged}(\mathrm{i}) + \mathrm{Pheating}_{Mannaged}(\mathrm{i}) \tag{53}$$

$$\mathrm{Correlation}(\mathrm{Psurplus}, \mathrm{Pload}_{Old}) = 0.35 \tag{54}$$

$$\mathrm{Correlation}(\mathrm{Psurplus}, \mathrm{Pload}_{New}) = 0.79 \tag{55}$$

where $\mathrm{Pcooling}_{\mathrm{Unmannaged}}$ and $\mathrm{Pheating}_{\mathrm{Unmannaged}}$ represent the cooling and heating load values before the application of the proposed load management method, and $\mathrm{Pcooling}_{\mathrm{Mannaged}}$ and $\mathrm{Pheating}_{\mathrm{Mannaged}}$ denote the cooling and heating loads after applying the load management strategy. The presented load management method increases the correlation between total load curve of the smart grid and the generated surplus power by renewable energy sources. This is shown by (53) and (54).

VIII. CONCLUSION

This paper sets forth a novel intelligent residential heating/cooling system controller that has smart grid functionality. In this paper, a possible implementation of an active controller will be examined. The optimization objective of the heating/cooling systems management is to minimize the cost of smart microgrid, the size of renewable energy resources, imported energy from distribution grid, and improve reliability of smart microgrid. Simulation studies show that managing the power consumption of heating and cooling systems based on the proposed method will decrease the size of renewable energy generators (wind and solar), increase the amount of stored hydrogen in the hydrogen tank, reduce the purchased power from distributed grid, increase the sold power to distributed grid, decrease the non-supply loads, purchased gas from utility and the total cost of smart microgrid.

The results demonstrate that smart heating/cooling system and renewable energy can work well together, and their individual benefits can be added together when used in combination.

REFERENCES

[1] A. Brooks, E. Lu, D. Reicher, C. Spirakis, and B. Weihl, "Demand dispatch," *IEEE Power Energy Mag.*, vol. 8, pp. 20–29, 2010.
[2] S. M. Hakimi and S. M. M. Tafreshi, "Optimization of smart microgrid considering domestic flexible loads," *J. Renewable Sustainable Energy*, vol. 4, pp. 1–15, 2012.
[3] S. M. Hakimi and S. M. M. Tafreshi, "Effect of plug-in hybrid electric vehicles charging/discharging management on planning of smart microgrid," *J. Renewable Sustainable Energy*, vol. 4, pp. 30–45, 2012.
[4] K. F. Fong, V. I. Hanby, and T. T. Chow, "HVAC system optimization for energy management by evolutionary programming," *Energy Build.*, vol. 38, pp. 220–231, 2008.
[5] W. Deng, W. Pei, and Z. Qi, "Impact and improvement of distributed generation on voltage quality in micro-grid," in *Proc. 3rd Int. Conf. Electric Utility Dereg. and Restruct. and Power Technol.*, 2008, pp. 1737–1741.
[6] R. H. Lasseter, "Microgrids," in *Proc. IEEE Power Eng. Soc. Winter Meeting*, 2002, vol. 1, pp. 305–308.
[7] C. Marnay and G. Venkataramanan, "Microgrids in the evolving electricity generation and delivery infrastructure," in *Proc. IEEE Power Eng. Soc. Winter Meeting*, 2006, pp. 18–22.
[8] N. Lu, "An evaluation of the HVAC load potential for providing load balancing service," *IEEE Trans. Smart Grid*, vol. 3, pp. 1263–1270, 2012.
[9] Y. Zhang and N. Lu, "Demand-side management of air conditioning cooling loads for intra-hour load balancing," in *Innovative Smart Grid Technol. (ISGT)*, 2013, pp. 1–6.
[10] N. Ruiz, "A direct load control model for virtual power plant management," *IEEE Trans. Power Syst.*, vol. 4, pp. 959–966, 2009.
[11] P. Jahangiri, W. Di, and C. Chengrui, "Intelligent residential air-conditioning system with smart-grid functionality," *IEEE Trans. Smart Grid*, vol. 3, pp. 2240–2251, 2012.
[12] Y. Hong, J. Kai Lin, C. Ping Wu, and C. Chuang, "Multi-objective air-conditioning control considering fuzzy parameters using immune clonal selection programming," *IEEE Trans. Smart Grid*, vol. 3, pp. 1603–1610, 2012.
[13] E. H. Mathews, C. P. Botha, D. C. Arndt, and A. Malan, "HVAC control strategies to enhance comfort and minimise energy usage," *Energy Build.*, vol. 33, pp. 853–863, 2001.
[14] N. Nassif, S. Kajl, and R. Sabourin, "Evolutionary algorithms for multi-objective optimization in HVAC system control strategy," in *Proc. IEEE Fuzzy Inf. Process. Soc. Annu. Meet.*, 2004, pp. 51–56.

[15] F. Calvino, M. La Gennusa, G. Rizzo, and G. Scaccianoce, "The control of indoor thermal comfort conditions: Introducing a fuzzy adaptive controller," *Energy Build.*, vol. 36, pp. 97–102, 2004.
[16] S. Ari, I. A. Cosden, H. E. Khalifa, J. F. Dannenhoffer, P. Wilcoxen, and C. Isik, "Constrained fuzzy logic approximation for indoor comfort and energy optimization," in *Proc. IEEE Fuzzy Inf. Process. Soc. Annu. Meet.*, 2005, pp. 500–504.
[17] A. I. Dounis and C. Caraiscos, "Advanced control systems engineering for energy and comfort management in a building environment-A review," *Renewable Sustainable Energy Rev.*, vol. 13, pp. 1246–1261, 2009.
[18] *Thermal Environmental Conditions for Human Occupancy*, ASHRAE Std. 55, 2010.
[19] M. Hamdi and G. Lachiver, "A fuzzy control system based on the human sensation of thermal comfort," in *Proc. IEEE World Congr. Comput. Intell.*, 1998, pp. 487–492.
[20] K. Chen, Y. Jiao, and E. S. Lee, "Fuzzy adaptive networks in thermal comfort," *Appl. Math. Lett.*, vol. 19, pp. 420–426, 2006.
[21] J. Liang and R. Du, "Thermal comfort control based on neural network for HVAC application," *IEEE Control Applicat.*, pp. 819–824, 2005.
[22] A. Faruqui and S. Sergici, "Household response to dynamic pricing of electricity: A survey of the empirical evidence," *J. Regulatory Econ.*, vol. 38, pp. 193–225, 2010.
[23] A. Rogers, S. Maleki, S. Ghosh, and N. R. Jennings, "Adaptive home heating control through Gaussian process prediction and mathematical programming," *Agent Technol. Energy Sys.*, pp. 71–78, 2010.
[24] R. T. Guttromson, D. P. Chassin, and S. E. Widergren, "Residential energy resource models for distribution feeder simulation," in *Proc. IEEE PES General Meeting*, 2003, pp. 108–113.
[25] D. P. Chassin, J. M. Malard, C. Posse, A. Gangopadhyaya, N. Lu, S. Katipamula, and J. V. Mallow, Modeling Power Systems as Complex Adaptive Systems Pacific Northwest National Laboratory, 2004, Tech. Rep..
[26] D. Hammerstrom, Pacific Northwest Gridwise Testbed Demonstration Projects-Part I Olympic Peninsula Project U.S. Department of Energy at Pacific Northwest National Laboratory, Tech. Rep., PNNL-17167, 2007.
[27] P. Constantopoulos, F. C. Schweppe, and R. C. Larson, "A real-time consumer control scheme for space conditioning usage under spot electricity pricing," *Comput. Operat. Res.*, vol. 18, pp. 751–765, 1991.
[28] D. J. Livengood, "The energy box: Comparing locally automated control strategies of residential electricity consumption under uncertainty," Ph.D. dissertation, Mass. Inst. Technol., Cambridge, MA, 2011.
[29] D. Molina, C. Lu, V. Sherman, and R. Harley, "Model predictive and genetic algorithm based optimization of residential temperature control in the presence of time-varying electricity prices," in *Industry Applicat. Soc. Annu. Meeting*, 2011, pp. 1–7.
[30] A. Aswani, N. Master, J. Taneja, D. Culler, and C. Tomlin, "Reducing transient and steady state electricity consumption in HVAC using learning-based model-predictive control," *IEEE J. Mag.*, vol. 100, pp. 240–253, 2012.
[31] F. I. Vázquez and W. Kastner, "Thermal Comfort Support Application for Smart Home Control," in *Ambient Intelligence-Software and Applications, Advances in Intelligent and Soft Computing*. New York, NY, USA: Springer, 2012, vol. 153, pp. 109–118.
[32] US Department of Energy Framework Public Meeting for Residential Central Air Conditioners and Heat Pumps pp. 35–36, 2008.
[33] H. Yang, W. Zhou, L. Lu, and Z. Fang, "Optimal sizing method for stand-alone hybrid solar-wind system with LPSP technology by using genetic algorithm," *Solar Energy*, vol. 82, pp. 354–367, 2008.
[34] R. Billinton and R. N. Allan, *Reliability Evaluation of Power Systems*. New York, NY, USA: Plenum, 1984.
[35] M. J. Khan and M. T. Iqbal, "Pre-feasibility study of stand-alone hybrid energy systems for applications in Newfoundland," *Renewable Energy*, vol. 38, pp. 835–854, 2005.
[36] M. Y. El-Sharkh, M. Tanrioven, A. Rahman, and M. S. Alam, "Cost related sensitivity analysis for optimal operation of a grid-parallel PEM fuel cell power plant," *J. Power Sources*, vol. 161, pp. 1198–1207, 2006.
[37] K. Strunz and E. K. Brock, "Stochastic energy source access management: Infrastructure-integrative modular plant for sustainable hydrogen-electric cogeneration," *Int. J. J Hydrogen Energy*, vol. 31, pp. 1129–1141, 2006.
[38] J. Kennedy and R. C. Eberhart, "Particle swarm optimization," in *IEEE Int. Conf. Neural Netw.*, 1995, pp. 1942–1948.
[39] Y. Shi and R. C. Eberhart, "A modified particle swarm optimizer," in *Proc. IEEE Int. Conf. Evolutionary Comput.*, 1998, pp. 69–73.
[40] Y. Shi and R. C. Eberhart, *Parameter Selection in Particle Swarm Optimization*. Berlin, Germany: Springer, 1998, vol. 1447, Lecture Notes in Computer Science, pp. 591–600.
[41] R. C. Eberhart and Y. Shi, "Comparing inertia weights and constriction factors in particle swarm optimization," *Congr. Evolutionary Comput.*, pp. 84–88, 2000.
[42] M. Clerc, "The swarm and the queen: Towards a deterministic and adaptive particle swarm optimization," *Congr. Evolutionary Comput.*, pp. 1951–1957, 1999.
[43] M. Lzvbjerg, T. K. Rasmussen, and T. Krink, "Hybrid particle swarm optimiser with breeding and subpopulations," in *Genetic and Evolutionary Computation Conf. (GECCO-2001)*, 2001.
[44] P. C. Fourie and A. A. Groenwold, "Particle swarms in algorithm in topology optimization," *FourthWorld Congress of Structural and Multidisciplinary Optimization*, pp. 52–53, 2001.
[45] A. Carlisle and G. Dozier, "Adapting particle swarm optimization to dynamic environments," in *Int. Conf. Artificial Intelligence*, 2000, pp. 429–434.
[46] J. Kennedy and R. C. Eberhart, "A discrete binary version of the particle swarm algorithm," in *Proc. Conf. Syst., Man Cybern.*, 1997, pp. 4104–4109.
[47] R. S. Garcia and D. Weisser, "A wind-diesel system with hydrogen storage: Joint optimization of design and dispatch," *Renewable Energy*, vol. 31, pp. 2296–2320, 2006.
[48] [Online]. Available: http://www.suna.org.ir/suna_content/media/image/2012/02/1455_orig.pdf

S. M. Hakimi, photograph and biography not available at the time of publication.

S. M. Moghaddas-Tafreshi, photograph and biography not available at the time of publication.